



## Biosynthesis, characterization, and antibacterial activity of gold nano particles

1. Mousumi Panda 2. B.B.BHOI 3. B.N.BISWAL

Nalanda Institute of Technology, Bhubaneswar

Dept. of Basic Science & Humanities

E-mail ID:mousumipanda@the nalanda.com

### ABSTRACT

**Background:** Due to rising bacterial resistance and adverse effects of antibiotics, research over the past few decades has centered on alternative antimicrobials. The current study looked at how well-chosen human pathogens responded to gold nanoparticles' antibacterial properties.

**METHODS:** In this study, gold nanoparticles were created using panchagavya (PG), and the resulting nanoparticles (PG-AuNPs) were then examined using various spectroscopic methods. Additionally, the well-diffusion method was used to assess the antibacterial activity of PG-AuNPs against *Escherichia coli*, *Bacillus subtilis*, and *Klebsiella pneumoniae*.

**Results:** A color change and a UV-Vis spectrum with a maximum absorption peak at 527 nm were used to confirm the synthesis of AuNPs. From the UV results, the Tauc method calculated the bandgap energy to be 2.13 eV. FTIR analysis reveals that the presence of).

---

### Introduction

Nanomaterials are becoming more widely used in medicine due to their drug delivery mechanism in cancer therapy, as well as their availability, material properties, and capacity to improve

---

drug selectivity against cancer cells [1]. Gold nanoparticles (AuNPs) have generated increased interest among diverse metallic nanoparticles because of their unique qualities, which include nano size, low toxicity, comparatively simple fabrication, and precise targeting [2]. The antibacterial property of AuNPs has recently been a major research topic, making them a good candidate for antibiotic complementation. The antibacterial activity of AuNPs is mediated by the development of holes in the bacterial cell wall, resulting in cell death due to the loss of cell contents. Furthermore, AuNPs can inhibit multidrug-resistant pathogens by attaching to bacte-

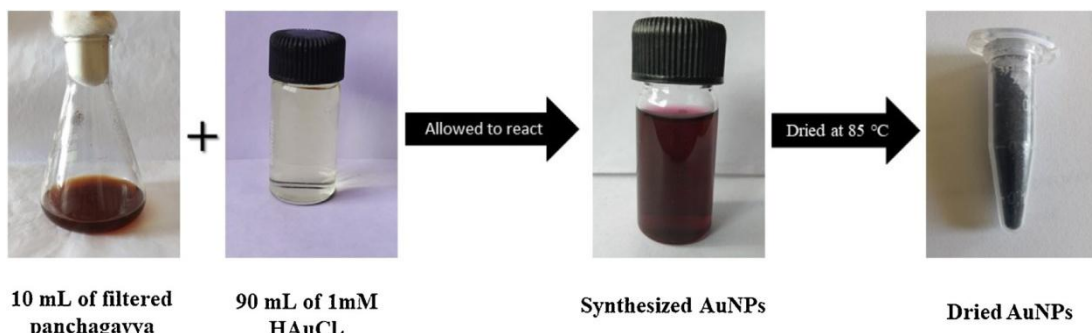


**Fig. 1.** Schematic diagram of panchagavya mediated gold nanoparticles.

rial DNA and blocking the uncoiling of DNA during transcription by binding to bacterial DNA [3]. For the synthesis of nanoparticles, a variety of technologies are used; among them, biological methods are less hazardous and environmentally benign.

The biological method was done by using bacteria, fungi, biomolecules, plants, and other natural raw materials for the synthesis of nanoparticles. Natural nanoparticles are employed as unique reducing and capping agents for the effective reduction of metallic ions into nanoparticles, whose chemistry is inextricably tied to the characteristics of the raw materials, resulting in a synergy between both materials [4]. *panchagavya* (PG) is a magnificent combination of five cow-derived products: urine, dung, milk, curd, and ghee. Importantly, PG is a mixture of microorganisms, including *Azotobacter* sp., *Azospirillum* sp., *Pseudomonas* sp., probiotics, and a variety of other beneficial organisms. Moreover, carbohydrates, proteins, lipids, micronutrients, and antioxidants are present in the PG. Silver and copper nanoparticles synthesized from PG showed significant antibacterial and free radicals scavenging activities respectively [5,6]. However, no report on the synthesis of AuNPs using panchagavya has been published till date. Hence, the current study will be established as a future reference for the further investigations on PG nanoparticles. The goal of this study was to synthesize and characterize AuNPs utilizing PG as well as evaluate the antibacterial activity of synthesized nanoparticles (PG-AuNPs) against *Escherichia coli*, *Bacillus subtilis*, and *Klebsiella pneumoniae*.

## Materials and methods

### *Preparation of panchagavya (PG)*

The procedure given by Gandhi et al., [6] was used to prepare the PG. The prepared PG was filtered using Whatman No 1 filter paper and the filtrate was used to synthesize AuNPs the schematic diagram as shown in Fig. 1.

Synthesis and characterization of AuNPs

For the genesis of AuNPs, 10 mL of PG extract was combined with 90 mL of HAuCl<sub>4</sub> (1 mM) and allowed to react at room temperature (RT); the colour of the reaction mixture varied over the incubation period, indicating the synthesis of AgNPs. UV-visible (UV-vis)



spectroscopy in the range of 300 nm–800 nm demonstrated the reduction of silver ions into AuNPs spectrophotometrically. The PG-AuNPs solution was spun for 40 min at 25,000 rpm to attain pure PG-AuNPs in a dry state for further analysis. For the Fourier transform infrared spectrometer (FTIR) study, the dried PG-AuNPs were mixed with KBr and formed into pellets. With a voltage of 30 kV and a current of 20 mA, X-ray diffraction (XRD) analysis of PG-AuNPs was investigated with a scan speed of 2.0°/min and a scan width of 0.02° within the scan range of 20°–80° (Bruker D8). The size and charge of the PG-AgNPs were determined using a SZ- 100 dynamic light scattering analyzer. Micrographs generated from high-resolution transmission electron microscopy (HRTEM) combined with energy dispersive X-ray spectroscopy (EDS) were used to analyse the particle shape and elemental content of PG-AuNPs.

#### *Antibacterial activity*

The antibacterial activity of PG-AuNPs was investigated using the standard well diffusion method against *Bacillus subtilis* (MTCC 2394), *E. coli* (MTCC 448), and *K. pneumoniae* (MTCC 109) [7]. Freshly formed culture was spread on sterilized nutrient agar plates, and 8 mm wells in the agar plates were made with a sterile cork borer. The wells were loaded with different concentrations (10 µL, 20 µL, 30 µL, and 40 µL) of PG-AuNPs and 10 µL of ciprofloxacin was serving as a control. After that, the plates were maintained at 37 °C for a day, and the antibacterial activity of the PG-AuNPs was determined by measuring zones of inhibition (ZOI) around the well impregnated with PG-AuNPs.

### **Results and discussion**

#### *UV analysis*

The shift in the colour of the solution from brown to ruby red verified the generation of PG-AuNPs [8]. UV-vis spectroscopic analysis is a widely used approach for determining the formation of metal nanoparticles by examining the unique optical properties of the nanoparticles, which are dependent on their size and shape [9]. The synthesized AuNPs are indicated by a prominent single surface plasmon resonance (SPR) band at 527 nm in the UV-vis spectra as shown in Fig. 2. The SPR band was developed when free electrons in PG-AuNPs were excited while absorbing visible light [10]. Spherical nanoparticles produce a single SPR band in the absorption spectra, according to Mie's theory [11]. Singh et al., [12] also reported a UV absorption peak at 527 nm for synthesized AuNPs nanoparticles using *Padina gymnospora*. The bandgap energy was determined from UV analysis using the Tauc plot method [13], and it was found to be 2.13 eV (Fig. 3). The low energy gap of PG-AuNPs ensures that visible light is adequately absorbed [14].

#### *FTIR analysis*

An infrared spectrum, which can be considered as a sample fingerprint by resulting absorption bands due to the bending or stretching of unique bonds. Different peaks were found in the FTIR spectra at  $3192\text{ cm}^{-1}$ ,  $2937\text{ cm}^{-1}$ ,  $1576\text{ cm}^{-1}$ ,  $1091\text{ cm}^{-1}$ ,  $1013\text{ cm}^{-1}$ , and  $857\text{ cm}^{-1}$  as shown in Fig. 4. The major stretching vibrations of the O H group were

found at  $3192\text{ cm}^{-1}$ . The band at

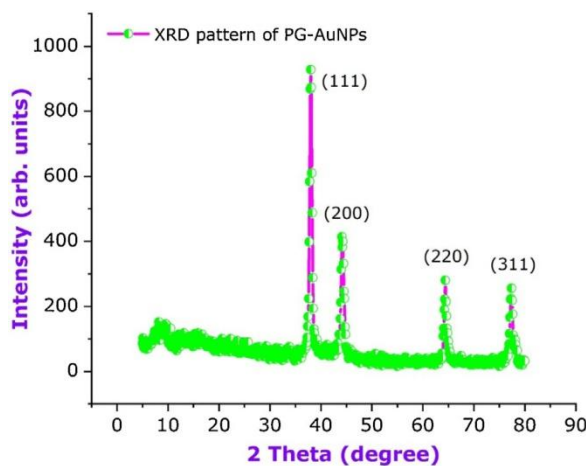
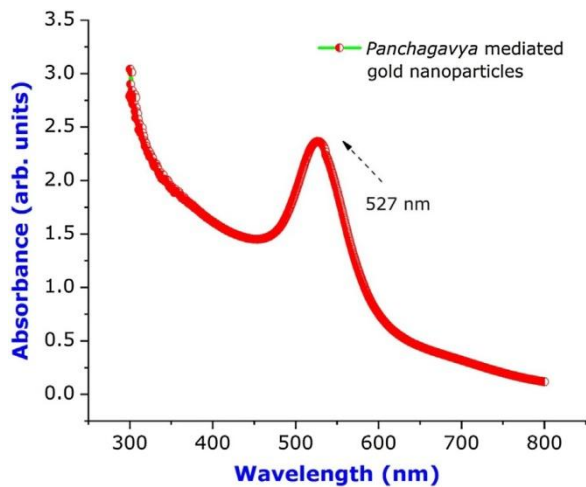


**Fig. 2.** UV-vis absorbance spectrum of panchagavya mediated AuNPs.

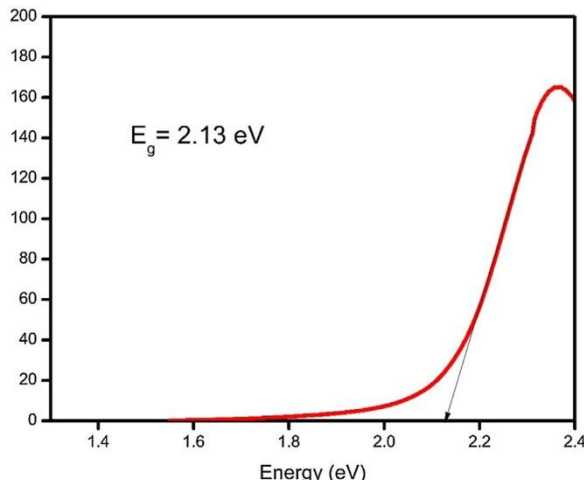


**Fig. 3.** Direct energy bandgap of panchagavya mediated AuNPs.

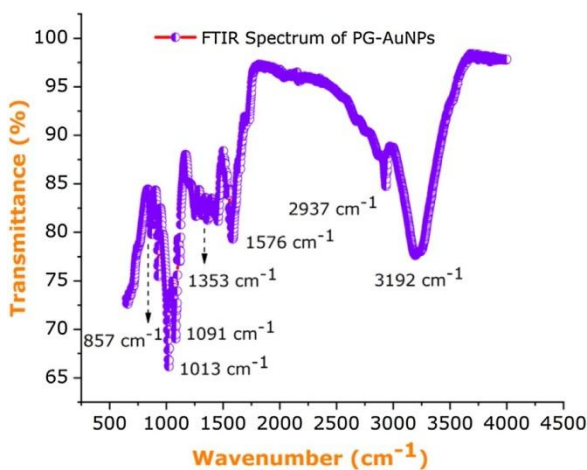


**Fig. 4.** FTIR spectrum of panchagavya mediated AuNPs.

$2937\text{ cm}^{-1}$  corresponded to the C-H stretch of the protein's methylene groups [15] and the C=C stretching of the benzene ring was observed at  $1576\text{ cm}^{-1}$  [16]. The NH stretch vibration occurring in the amide bonds of the proteins was ascribed to the band at  $1462\text{ cm}^{-1}$ . The NO symmetry stretching characteristic of the nitro compound is exemplified by the band at  $1364\text{ cm}^{-1}$ . The small

**Fig. 5.** XRD pattern of panchagavya mediated AuNPs.

band at  $1246\text{ cm}^{-1}$  representing CN stretching of amines [17]. Secondary alcohols

and/or the C-O- stretching ester group would be linked to a band at  $1091\text{ cm}^{-1}$  and  $924\text{ cm}^{-1}$  [18,19]. The CN stretching vibrations of aromatic and aliphatic amines are responsible for the band detected at  $1013\text{ cm}^{-1}$  [20]. NH<sub>2</sub> primary amines were found in the band at  $857\text{ cm}^{-1}$ . According to the FTIR results, amino acids and proteins have a greater ability to adhere to metal and are involved in the depletion and capping of AuNPs in the liquid media [21].

#### *Phase analysis (XRD)*

XRD is primarily used to identify phases and characterize the crystalline nature of PG-AuNPs. Fig. 5. illustrates the face-centered cubic (FCC) AuNPs because of XRD analysis, which is agreed with the FCC structure referenced in joint committee of powder diffraction standard (JCPDS) card no. 04-0784 [22]. Furthermore, the XRD peaks at  $2\theta$  of  $38.30^\circ$ ,  $44.67^\circ$ ,  $64.57^\circ$ , and  $78.76^\circ$  might be assigned to the (111), (200), (220), and (311) crystallographic planes, indicating that the PG-AuNPs are cubic crystalline. These findings corroborate a previous report on the manufacture of gold nanoparticles by endophytic bacteria [23].

#### *Dynamic light scattering studies (DLS) Particle size*

The hydrodynamic size and zeta potential of nanoparticles are significant features for future uses in nanoparticle research. The hydrodynamic size was determined to be 53.29 nm with a polydispersity index of 0.354, as illustrated in Fig. 6(a). The value of the polydispersity index is less than 0.7, indicating that the nanoparticles are of good quality. Similarly, Khandel et al., [24] found that the average size of *Alpinia calcarata* leaf extract mediated AgNPs was

45.2 nm, with a polydispersity index of 0.258, indicating that the nanoparticles were of acceptable quality.

#### *Zeta potential analysis*

A high absolute zeta potential value suggests that the nanoparticles have a large electric charge on their surface. It defines the particle's strong repelling forces, which prevent aggregation and stabilize Nanoparticles in the buffer solution. The zeta potential was discovered to be 9.8 mv in Fig. 6(b). Due to electrostatic repulsion, it was concluded that gold nanoparticles had warped with anionic substances and that the particles were relatively stable [25].

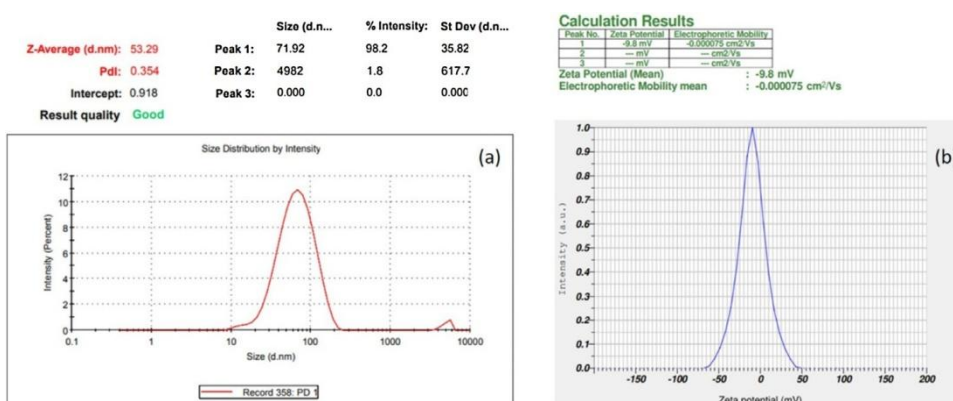


**Fig. 6.** (a) DLS analysis of particle size and; (b) Zeta potential of PG-AuNPs.

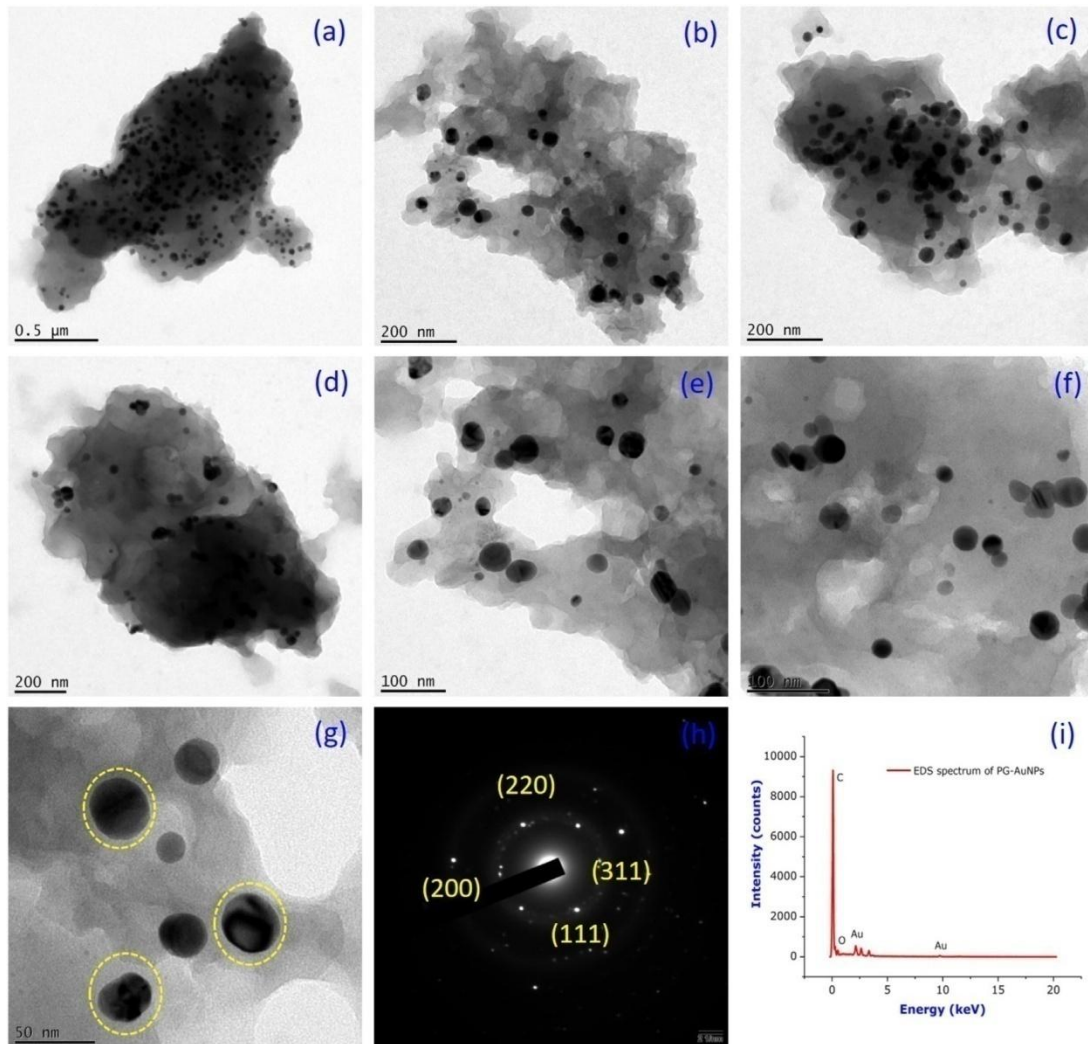


**Fig. 7.** HRTEM analysis of PG-AuNPs. (a-g) Spherical shaped PG-AuNPs; (h) SAED pattern of PG-AuNPs; (i) EDS spectrum of PG-AuNPs.

**Table 1**

ZOI of tested bacterial strains at different concentration of PG. The results were expressed as mean + standard deviation.

Strain	$ZOI^{(mm)}$	Control (10 $\mu$ L)	10 $\mu$ L	20 $\mu$ L	30 $\mu$ L	40 $\mu$ L
<i>B. subtilis</i>		$12.33 \pm 0.17$	$9.17 \pm 0.17$	$9.33 \pm 0.33$	$10.16 \pm 0.17$	$11.42 \pm 0.58$
<i>E. coli</i>		$14.33 \pm 0.53$	$9.33 \pm 0.17$	$10.16 \pm 0.17$	$11.17 \pm 0.33$	$12.67 \pm 0.24$

<i>K. pneumoniae</i>	$26 \pm 0.57$	$13.16 \pm 0.17$	$13.33 \pm 0.17$	$15.17 \pm$
	$0.3317.12 \pm 0.14$			

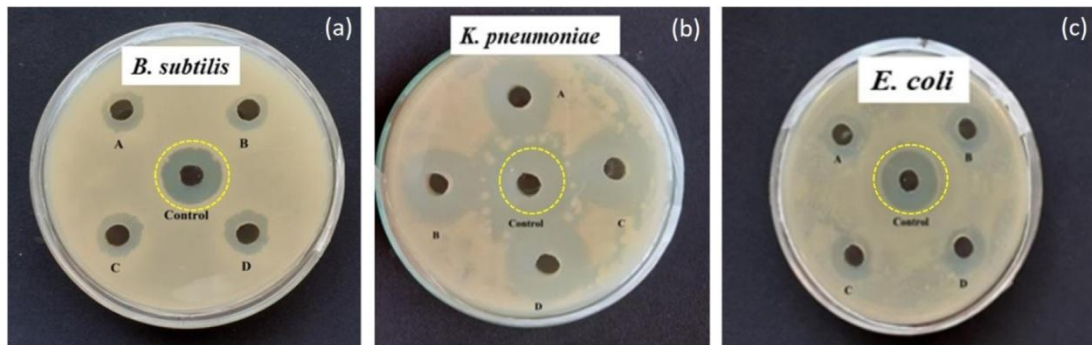


**Fig. 8.** Antibacterial activity of PG-AuNPs against gram-positive and gram-negative organisms at 10  $\mu\text{L}$  (A), 20  $\mu\text{L}$  (B), 30  $\mu\text{L}$  (C) and 40  $\mu\text{L}$  (D). *Bacillus subtilis* (MTCC 2394), *E. coli* (MTCC 448), and *K. pneumoniae*.

#### High resolution transmission electron microscopy (HRTEM)

HRTEM analysis was used to evaluate the morphology of gold nanoparticles [26]. The image of PG-AuNPs with a spherical shape was given in Fig. 7(a-i), EDS analysis of PG-AuNPs showed strong signals corresponding to gold along with weak signals corresponding to oxygen in Fig. 7(i). The weak signals are raised from macromolecules in the PG extract, such as proteins/enzymes and salts [27]. The results are consistent with previous reports of gold nanoparticles discovered using various synthesis methods [28,29]. Selected area electron diffraction (SAED) of nanoparticles revealed the crystalline nature of the PG-AuNPs yet again. Bright circular pattern rings were discovered in this study. The PG-AuNPs in cubic crystal form was also indicated by circular patterns of spots matching to reflections from the (111), (200), (220), and (311) of lattice planes as shown in Fig. 7(h). Our findings were in line with those of Doan et al., [15] and Qian et al., [29].

#### Antibacterial activity

The antibacterial activity of PG-AuNPs against selected bacterial strains were displayed in Fig. 8(a-c). The acquired result showed that the PG-AuNPs were harmful to all the tested bacterial strains at various doses. Among the bacterial strain examined, PG-AuNPs exhibited the strongest inhibitory activity against *K. pneumoniae* followed by *E. coli*, and *B. subtilis* with ZOI of  $17.12 \pm 0.14$ ,  $12.67 \pm 0.24$ , and  $11.42 \pm 0.58$  mm, respectively at the highest concentration (40  $\mu\text{L}$ ) Table 1. When metal ions in solution come into contact with a bacterial cell, they become generally dispersed in the environment around the bacterial cell, with no specific localisation. NPs that engage with the bacterial cell wall, on the other hand, form a focused source of ions that constantly release ions, increasing cell toxicity [30]. Our findings showed that the PG-AuNPs have a better antibacterial effect against gram-negative bacteria. This could be because gram-positive bacteria has strong cell wall, whereas gram-negative bacteria has thin cell wall so the PG-AuNPs easily



penetrate to the cell membrane of the gram-negative bacteria and causes damages to the cell [31,32]. The antibacterial property of gold NPs was achieved in two processes. They inhibited the metabolic process by changing the membrane potential and lowering adenosine triphosphate (ATP) synthase activity. Second, they rejected the ribosome's subunit for tRNA binding, effectively dismantling its biological process. They were also found to be less harmful to mammalian cells [33]. Gold nanoparticles in various dimensions and shapes are the most widely investigated nano-materials for antibacterial and anti-biofilm applications, according to a recent literature review [34]. Electronic effects are produced by gold NPs with a small size and increased surface area, which are advantageous for increasing the surface reactivity of NPs. Furthermore, the high surface area percentage immediately interacted with the bacterium to a large amount, resulting in improved bacteria interaction. The antibacterial activity of the NPs with large surface area was considerably increased by these two critical features [35]. Previous research has shown that gold nanoparticles play an important role in drug delivery and can be used to combat a wide range of pathogenic bacteria due to their effective antibacterial properties [36–38]. The findings suggest that PG-AuNPs may be a useful tool for antibacterial drug for now and in the future.

## Conclusion

In conclusion, we discovered that AuNPs were successfully synthesized utilizing PG as a reducing agent, and they were characterized using various techniques. The formation of AuNPs was primarily detected when the colour solution changed, and UV absorption spectra revealed a maximum absorbance peak at 527 nm. The FTIR data revealed PG-AuNPs with a variety of functional groups includes amino acids and proteins. XRD, SAED, TEM, and DLS displayed crystalline nature, spherical morphology, elemental composition, and the particle size was discovered to be 53.29 nm. The synthesized nanoparticles showed a higher and moderate antibacterial activity against gram negative and gram-positive bacteria respectively.

## Funding

No funding sources.

## Competing interests

None declared.

## Ethical approval

Not required.

## Acknowledgment

The authors acknowledge Department of Biotechnology, Thiruvalluvar University, Serkkadu, Vellore, India for providing facilities to carry out the research work. Also, the authors extend their appreciation to the Researchers supporting project number (RSP-2021/189), King Saud University, Riyadh, Saudi Arabia.



## References

- [1] Liu F, Ma D, Chen W, Chen X, Qian Y, Zhao Y, et al. Gold nanoparticles suppressed proliferation, migration, and invasion in papillary thyroid carcinoma cells via downregulation of CCT3. *J Nanomater* 2019;2019.
- [2] Fu LH, Yang J, Zhu JF, Ma MG. Synthesis of gold nanoparticles and their applications in drug delivery. In: Metal nanoparticles in pharma. Cham: Springer; 2017. p. 155–91.
- [3] Arafa MG, El-Kased RF, Elmazar MM. Thermoresponsive gels containing gold nanoparticles as smart antibacterial and wound healing agents. *Sci Rep* 2018;8(1):1–6.
- [4] Saravanan M, Vahidi H, Cruz DM, Vernet-Crua A, Mostafavi E, Stelmach R, et al. Emerging antineoplastic biogenic gold nanomaterials for breast cancer therapeutics: a systematic review. *Int J Nanomed* 2020;15:3577.
- [5] Govarthanan M, Selvankumar T, Manoharan K, Rathika R, Shanthi K, Lee KJ, et al. Biosynthesis and characterization of silver nanoparticles using panchakavya, an Indian traditional farming formulating agent. *Int J Nanomed* 2014;9:1593.
- [6] Arumugam DG, Sivaji S, Dhandapani KV, Nookala S, Ranganathan B. Panchagavya mediated copper nanoparticles synthesis, characterization and evaluating cytotoxicity in brine shrimp. *Biocatal Agric Biotechnol* 2019;19:101132.
- [7] Sathiyaraj S, Suriyakala G, Gandhi AD, Saranya S, Santhoshkumar M, Kavitha P, et al. Green biosynthesis of silver nanoparticles using vallarai chooranam and their potential biomedical applications. *J Inorg Organomet Polym Mater* 2020;30(11):4709–19.
- [8] ElMitwalli OS, Barakat OA, Daoud RM, Akhtar S, Henari FZ. Green synthesis of gold nanoparticles using cinnamon bark extract, characterization, and fluorescence activity in Au/eosin Y assemblies. *J Nanopart Res* 2020;22(10):1–9.
- [9] Paulkumar K, Gnanajobitha G, Vanaja M, Pavunraj M, Annadurai G. Green synthesis of silver nanoparticle and silver based chitosan bionanocomposite using stem extract of *Saccharum officinarum* and assessment of its antibacterial activity. *Adv Nat Sci-Nanosci* 2017;8:035019.
- [10] Baia L, Muresan D, Baia M, Popp J, Simon S. Structural properties of silver nanoclusters–phosphate glass composites. *Vib Spectrosc* 2007;43(2):313–8.
- [11] Eya’ane Meva F, Segnou ML, Ebongue CO, Ntoumba AA, Kedi PB, Deli V, et al. Spectroscopic synthetic optimizations monitoring of silver nanoparticles formation from *Megaphrynum macrostachyum* leaf extract. *Rev Bras Farmacogn* 2016;26:640–6.
- [12] Singh M, Kalaivani R, Manikandan S, Sangeetha N, Kumaraguru AK. Facile green synthesis of variable metallic gold nanoparticle using *Padina gymnospora*, a brown marine macroalga. *Appl Nanosci* 2013;3(2):145–51.
- [13] Ramesh R, Catherine G, Sundaram SJ, Khan FL, Kaviyarasu K. Synthesis of Mn<sub>3</sub>O<sub>4</sub> nano complex using aqueous extract of *Helianthus annuus* seed cake and its effect on biological growth of *Vigna radiata*. *Mater Today: Proc* 2021;36:184–91.
- [14] Raja A, Selvakumar K, Rajasekaran P, Arunpandian M, Ashokkumar S, Kaviyarasu K, et al. Visible active reduced graphene oxide loaded titania for



photodecomposition of ciprofloxacin and its antibacterial activity. *Colloids Surf A Physicochem Eng Asp* 2019;564:23–30.

- [15] Doan VD, Huynh BA, Nguyen TD, Cao XT, Nguyen VC, Nguyen TL, et al. Biosynthesis of silver and gold nanoparticles using aqueous extract of *Codonopsis pilosula* roots for antibacterial and catalytic applications. *J Nanomater* 2020;2020.
- [16] Devi TA, Ananthi N, Amaladhas TP. Photobiological synthesis of noble metal nanoparticles using *Hydrocotyle asiatica* and application as catalyst for the photodegradation of cationic dyes. *J Nanostructure Chem* 2016;6(1):75–92.
- [17] Mani M, Harikrishnan R, Purushothaman P, Pavithra S, Rajkumar P, Kumaresan S, et al. Systematic green synthesis of silver oxide nanoparticles for antimicrobial activity. *Environ Res* 2021;202:111627.
- [18] Oliveira RN, Mancini MC, Oliveira FC, Passos TM, Quilty B, Thiré RM, et al. FTIR analysis and quantification of phenols and flavonoids of five commercially available plants extracts used in wound healing. *Matéria (Rio J)* 2016;21:767–79.
- [19] Mani M, Pavithra S, Mohanraj K, Kumaresan S, Alotaibi Saqer S, Eraqi Mostafa M, et al. Studies on the spectrometric analysis of metallic silver nanoparticles (Ag NPs) using *Basella alba* leaf for the antibacterial activities. *Environ Res* 2021;199:111274.
- [20] Mani M, Okla Mohammad K, Selvaraj S, Ram Kumar A, Kumaresan S, Muthukumaran Azhaguchamy, et al. A novel biogenic *Allium cepa* leaf mediated silver nanoparticles for antimicrobial, antioxidant, and anticancer effects on MCF-7 cell line. *Environ Res* 2021;198:111199.
- [21] Suriyakala G, Sathiyaraj S, Gandhi AD, Vadakkan K, Rao UM, Babujanarthanam R. *Plumeria pudica* Jacq. flower extract-mediated silver nanoparticles: characterization and evaluation of biomedical applications. *Inorg Chem Commun* 2021;126:108470.
- [22] Sant DG, Gujarathi TR, Harne SR, Ghosh S, Kitture R, Kale S, et al. *Adiantum philipense* L. frond assisted rapid green synthesis of gold and silver nanoparticles. *J Nanoparticle* 2013;2013.
- [23] Syed B, Prasad NM, Satish S. Endogenic mediated synthesis of gold nanoparticles bearing bactericidal activity. *J Microsc Ultrastruct* 2016;4:162–6.
- [24] Khandel P, Shahi SK, Soni DK, Yadaw RK, Kanwar L. *Alpinia calcarata*: potential source for the fabrication of bioactive silver nanoparticles. *Nano Converg* 2018;5:37.
- [25] Shabestarian H, Homayouni-Tabrizi M, Soltani M, Namvar F, Azizi S, Mohamad R, et al. Green synthesis of gold nanoparticles using sumac aqueous extract and their antioxidant activity. *Mater Res* 2017;20:264–70.
- [26] Paramanantham P, Antony AP, Lal SS, Sharan A, Syed A, Ahmed M, et al. Antimicrobial photodynamic inactivation of fungal biofilm using amino functionalized mesoporous silica-rose bengal nanoconjugate against *Candida albicans*. *Sci Afr* 2018;1:e00007.
- [27] Bathrinarayanan PV, Thangavelu D, Muthukumarasamy VK, Munusamy C, Gurunathan B. Biological synthesis and characterization of intracellular gold nanoparticles using biomass of *Aspergillus fumigatus*. *Bull Mater Sci* 2013;36:1201–5.
- [28] Azizah N, Hashim U, Arshad MM, Gopinath SC, Nadzirah S, Farehanim MA, et al. Analysis study of single gold nanoparticle system of interdigitated device electrodes (ides) by using energy-dispersive x-ray (EDX). *ARPN J Eng Appl Sci* 2016;11.



- [29] Qian L, Su W, Wang Y, Dang M, Zhang W, Wang C. Synthesis and characterization of gold nanoparticles from aqueous leaf extract of *Alternanthera sessilis* and its anticancer activity on cervical cancer cells (HeLa). *Artif Cells Nanomed Biotechnol* 2019;47:1173–80.
- [30] Katas H, Lim CS, Azlan AY, Buang F, Busra MF. Antibacterial activity of biosynthesized gold nanoparticles using biomolecules from *Lignosus rhinocerotis* and chitosan. *Saudi Pharm J* 2019;27:283–92.
- [31] Slavin YN, Asnis J, Häfeli UO, Bach H. Metal nanoparticles: understanding the mechanisms behind antibacterial activity. *J Nanobiotechnology* 2017;1:1–20.
- [32] Parasuraman P, Antony AP, Sharan A, Siddhardha B, Kasinathan K, Bahkali NA, et al. Antimicrobial photodynamic activity of toluidine blue encapsulated in mesoporous silica nanoparticles against *Pseudomonas aeruginosa* and *Staphylococcus aureus*. *Biofouling* 2019;35(1):89–103.
- [33] Parasuraman P, Anju VT, Lal SS, Sharan A, Busi S, Kaviyarasu K, et al. Synthesis and antimicrobial photodynamic effect of methylene blue conjugated carbon nanotubes on *E. coli* and *S. aureus*. *Photochem Photobiol Sci* 2019;18(2):563–76.
- [34] Cui Y, Zhao Y, Tian Y, Zhang W, Lü X, Jiang X. The molecular mechanism of action of bactericidal gold nanoparticles on *Escherichia coli*. *Biomaterials* 2012;33:2327–33.
- [35] Okkeh M, Bloise N, Restivo E, De Vita L, Pallavicini P, Visai L. Gold nanoparticles: can they be the next magic bullet for multidrug-resistant bacteria? *Nanomaterials* 2021;11(2):312.
- [36] Shamaila S, Zafar N, Riaz S, Sharif R, Nazir J, Naseem S. Gold nanoparticles: an efficient antimicrobial agent against enteric bacterial human pathogen. *Nanomaterials* 2016;6(4):71.
- [37] González-Ballesteros N, Rodríguez-Argüelles MC, Lastra-Valdor M, González-Mediero G, Rey-Cao S, Grimaldi M, et al. Synthesis of silver and gold nanoparticles by *Sargassum muticum* biomolecules and evaluation of their antioxidant activity and antibacterial properties. *J Nanostructure Chem* 2020;10(4):317–30.
- [38] Folorunso A, Akintelu S, Oyebamiji AK, Ajayi S, Abiola B, Abdusalam I, et al. Biosynthesis, characterization and antimicrobial activity of gold nanoparticles from leaf extracts of *Annona muricata*. *J Nanostructure Chem* 2019;9(2):111–7.